

LOW-ASPECT-RATIO FLAT-SHIP THEORY

E. O. Tuck  
University of Adelaide

Visiting Professor of Fluid Mechanics  
The University of Michigan  
Academic Year 1972-73

This research was carried out under the  
Naval Ship Systems Command  
General Hydromechanics Research Program  
Subproject SR 009 01 01, administered by the  
Naval Ship Research and Development Center.  
Contract No. N00014-67-A-0181-0052

Reproduction in whole or in part permitted  
for any purpose of the United States Government

Approved for public release; distribution unlimited



Department of Naval Architecture  
and Marine Engineering  
College of Engineering  
The University of Michigan  
Ann Arbor, Michigan 48104

an alternative treatment of this class of expansion, for general hull shapes. In particular, we demonstrate very strong effects of gravity near the center plane of pointed bodies.

We also observe that at all Froude numbers, the low-aspect-ratio flat-ship integral equation possesses a "similarity" solution, such that the pressure distribution has the same shape at all stations. This linearized but gravity-dependent result should not be confused with the well-known conical similarity solution for non-linear planing or water entry in the absence of gravity (Gilbarg, (1960), p. 360). In fact the present geometrical requirement is for a cusped parabolic waterplane shape but an arbitrary section shape, whereas the non-linear zero-gravity solution requires a triangular plan form and section shape.

The low-aspect-ratio flat-ship integral equation is amenable to direct computation, and we present here some preliminary examples of its numerical solution. Much more work needs to be done to derive efficient procedures, and the present computer program can only be considered as a crude first attempt. However, the results are of considerable interest, indicating rather dramatic gravity effects especially near the center plane, as predicted analytically, and confirming Maruo's (1967) estimate of the lift coefficient of a delta wing at sufficiently high Froude number.

## 2. The General Flat Ship Problem

We use a rather unconventional co-ordinate system  $(x,y,s)$ , as in Tuck and von Kerczek (1968) and as sketched in Figure 1. The ship is supposed fixed with its bow at  $s=0$  and stern at  $s=L$  in a stream  $U$ . Thus the total flow field velocity is

$$\underline{q} = \underline{\nabla}(Us + \phi) , \quad (2.1)$$

where  $\phi$  is the perturbation velocity potential.

The body equation is

$$y = \eta(x,s) , \quad (2.2)$$

where  $\eta$  is generally expected to be negative, " $-\eta$ " being the depth of the buttock line  $x=\text{constant}$  at station  $s$ . Equation (2.2) is supposed to hold for

$$|x| < b(s) , \quad (2.3)$$

where  $b(s)$  is the half-waterplane width at station  $s$ . For  $|x| > b$  we may suppose that (2.2) defines the water surface elevation. The hull boundary condition is

$$\phi_y = (U + \phi_s)\eta_s + \phi_x \eta_x , \quad (2.4)$$

to be applied on the exact hull surface  $y=\eta$ .

We first make the small-draft approximation, introducing a small parameter  $\alpha$  measuring the draft/length ratio. Keeping only leading order terms with respect to  $\alpha$ , the boundary condition (2.4) reduces to

$$\phi_y = U\eta_s , \quad \text{on } y = 0. \quad (2.5)$$

It is important to note that the small- $\alpha$  approximation is a regular one, as distinct from the (potentially) singular perturbation represented by the small- $\epsilon$  slenderness approximation to be applied next, where  $\epsilon$  measures the beam/length ratio. We shall assume that  $\alpha \ll \epsilon$  so that (2.5) may be taken to hold quite accurately when we come to make the small  $\epsilon$  approximation.\*

---

\*It is of interest to note that, according to Acosta and DeLong (1971), the infinite-Froude-number slender-planing-surface analysis of Tulin (1956) is valid in the opposite limit  $\epsilon \ll \alpha$ .

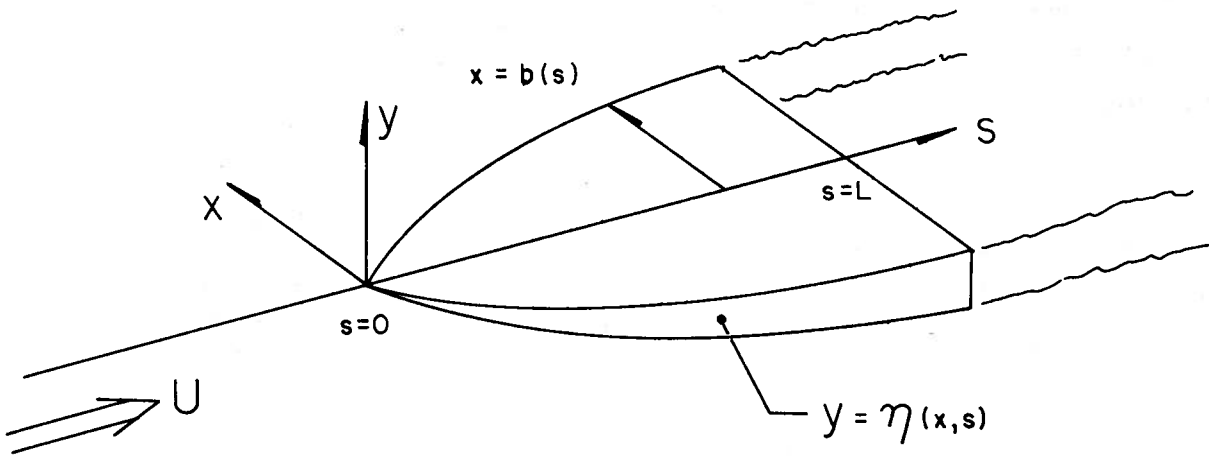


Figure 1: Sketch of Co-ordinate System

The boundary condition (2.4) also correctly gives the exact kinematic condition on the unknown free surface  $y=\eta$  for  $|x| > b$ . This has to be supplemented by the dynamic condition

$$\frac{P}{\rho} + U\phi_s + \frac{1}{2} |\nabla\phi|^2 + g\eta = 0, \quad (2.6)$$

if the excess of pressure over atmospheric at the free surface is  $P$ ; usually  $P=0$ . Again, the small-draft approximation enables linearization not only of (2.4) but also of (2.6) to give

$$\frac{P}{\rho} + U\phi_s + g\eta = 0, \quad \text{on } y = 0, \quad (2.7)$$

which combines with (2.5) to give the linearized free-surface condition

$$g\phi_y + U^2\phi_{ss} = -\frac{U}{\rho} P_s. \quad (2.8)$$

If  $P=0$ , this reduces to the usual equation

$$g\phi_y + U^2\phi_{ss} = 0. \quad (2.9)$$

However, we shall generate solutions by means of pressure distributions  $P$ , the velocity potentials then satisfying (2.8) whenever  $P \neq 0$ . Note that (2.9) results from the small- $\alpha$  approximation, and that alone; when we subsequently take  $\epsilon$  as small, (2.9) may be considered as exact.

The general flat-ship problem, with  $\epsilon$  not necessarily small, is that of solving the full Laplace equation

$$\phi_{xx} + \phi_{yy} + \phi_{ss} = 0 \quad (2.10)$$

in the space  $y < 0$ , subject to the hull condition (2.5) on the portion  $|x| < b(s)$  of the plane  $y=0$  occupied by the projection of the hull, and the linearized free-surface condition (2.9) on the portion  $|x| > b(s)$ . In addition we expect to require some kind of radiation condition at infinity, and a Kutta-type condition that the pressure reduces to atmospheric pressure at any sharp trailing edge in order that the free surface leave such an edge smoothly.

This problem can be converted into an integral equation, which is the finite-Froude-number analogue of the lifting-surface integral equation of aerodynamics. Maruo (1967) gives one method for accomplishing this; perhaps more directly we may set ourselves the task of finding an unknown surface pressure distribution  $P(x,s)$  which generates the free-surface

displacement  $\eta(x,s)$ . The corresponding integral connection\* between  $P$  and  $\eta$  may be obtained from well-known formulae, e.g. Wehausen and Laitone 1960, p. 598. For example

$$\pi^2 \rho U^2 \eta_s(x,s) = -Im \iint_W d\xi d\sigma P(\xi,\sigma) \int_0^{\pi/2} d\theta \sec\theta \quad (2.11)$$

$$\cdot \int_0^{\infty} dk \frac{k^2 e^{-ik(s-\sigma)} \cos\theta \cos(k(x-\xi)\sin\theta)}{k - \frac{g}{U^2} \sec^2\theta} ,$$

where the path of  $k$ -integration goes above the pole.

We shall not attempt to solve this integral equation here, since our concern is with the low-aspect-ratio case. However, several questions are worth noting. Maruo (1967) states that "the kernel of the integral equation is complicated enough to frustrate any attempt at solving it." This view is perhaps a little too pessimistic. The kernel is simply the complete solution for a travelling three-dimensional pressure point, and a number of similar computations have been carried out on an ad hoc basis recently (e.g. Monacella and Newman (1967), Gadd (1969), and van Oortmerssen (1972)). Of course there is more to the solution of the integral equation than just evaluating its kernel; however, direct numerical attack on this general flat-ship problem would seem worthwhile, and some effort is being put into this.

The role of the Kutta, or constant-pressure, condition at the trailing edge is worth comment. There is a degree of non-uniqueness about the integral equation (2.11); the homogeneous equation with  $\eta_s=0$  has a non-trivial set of solutions. This is illuminated by performing an indefinite  $s$ -integration of (2.11), introducing thereby an arbitrary function of  $x$  on the left-hand side, say  $C(x)$ . The resulting integrated operator permits a unique solution, the non-uniqueness being now absorbed into  $C(x)$ . This unknown function must

---

\*An interesting physical interpretation of this connection is the statement: "Every planing surface is hydrodynamically equivalent to some hovercraft." The equivalent hovercraft does not, of course, have a uniform base pressure.

somehow be determined by the requirement that  $P(x,s)$  vanishes at the trailing edge. Physically, this indeterminateness is equivalent to a degree of indeterminateness about the vertical location of the hull, and indeed at infinite aspect ratio ( $\frac{\partial}{\partial x} \equiv 0$ ),  $C$  is a constant, reflecting bodily upward or downward shift of the original given foil relative to the undisturbed free surface at infinity.

The zero- and infinite-Froude-number limits of (2.11) are of interest. In the zero-Froude-number case we obtain simply

$$P(x,s) = -\rho g \eta(x,s), \quad (2.12)$$

i.e., the appropriate pressure is hydrostatic. This is the apparent basis for the original flat-ship formula of Hogner (see Havelock, (1932)) which is however inconsistent, if used in a wave-resistance calculation at finite Froude number. At infinite Froude number, the integral equation reduces exactly to that of aerodynamic lifting-surface theory, so that the ship is equivalent to a lifting wing with camber surface  $y=\eta(x,s)$ . The role played by the Kutta condition is mathematically the same; it eliminates a degree of non-uniqueness in the general solution of the integral equation.

The analogy between the flat-ship theory and lifting-surface theory, which becomes an exact equivalence at  $g=0$ , illustrates a disturbing feature of the low-aspect-ratio flat-ship theory, namely that we shall not in general be able to satisfy the Kutta condition once the low-aspect-ratio approximation has been made. That is, the pressure predicted by the low-aspect-ratio theory at the edge of the transom stern will not in general be atmospheric. This would be a most unfortunate conclusion, were it not for the fact that low-aspect-ratio wing theory also suffers from this deficiency, yet nevertheless has proved useful. What presumably happens is that in a small neighborhood of the trailing edge there is a rapid change of pressure back to atmospheric. The hope is that this occurs over a dynamically-insignificant portion of the total hull and has no significant upstream effect. Some work has been done (e.g. Rogallo, (1970)) on the corresponding aerodynamic problem.

### 3. Derivation of the Low-Aspect-Ratio Flat-Ship Integral Equation

We now assume that the hull has a low aspect ratio, i.e. that it is slender, in the sense that its beam  $B$  is much smaller than its length  $L$ , say  $B=O(\epsilon) \cdot L$ . Note however that there is a definite heirachy of smallness in this problem, thus

$$\text{"Draft} \ll \text{Beam} \ll \text{Length} \text{"}.$$

The case when the draft and beam are comparable gives ordinary slender-ship theory, as in Tuck (1964) for low-to-moderate Froude numbers, and Ogilvie (1967) for moderate-to-high Froude numbers.

In the present case we are going to treat moderate-to-high Froude numbers, such that

$$v = \frac{gL^2}{U^2B} \tag{3.1}$$

is of order unity. This means that the conventional length-based Froude number is large, specifically

$$F = \frac{U}{\sqrt{gL}} = O(\sqrt{L/B}) = O(\epsilon^{-\frac{1}{2}}). \tag{3.2}$$

This is the regime treated by Ogilvie (1967) and by Maruo (1967).

In fact the appropriate integral equation can be obtained by specializing Ogilvie's (1967) inner problem, for the case of small draft/beam ratio. Ogilvie's (1967) general problem requires solution of a non-linear two-dimensional free-surface problem in each cross-section. The small-draft approximation linearizes this problem and can lead to the same integral equation as is obtained by the reverse procedure, i.e. of "small  $\alpha$ , then small  $\epsilon$ ," rather than "small  $\epsilon$ , then small  $\alpha$ ".

Since the body is slender, we expect as usual to have to solve a two-dimensional problem in the  $(x,y)$  cross-flow plane, i.e. dropping  $\phi_{ss}$  from the Laplace equation (2.10) to give

$$\phi_{xx} + \phi_{yy} = 0 \tag{3.3}$$

In the Froude-number range in which  $v=O(1)$  it is clear that both terms in the free-surface condition (2.9) must be retained, since  $\frac{\partial}{\partial s} = O(L^{-1})$  and  $\frac{\partial}{\partial y} = O(B^{-1})$ .



If we temporarily define a "pseudo-time" co-ordinate  $t$  by the equation

$$s = Ut, \quad (3.4)$$

the free-surface condition (2.9) becomes

$$g\phi_y + \phi_{tt} = 0 \quad (3.5)$$

which is identical to the usual unsteady linearized free-surface condition for water waves. Thus, since  $\phi$  now satisfies (3.3), not (2.10), we can use any solution for unsteady two-dimensional linearized water waves, replacing  $t$  by  $s/U$ .

The solution of most direct use is again that of a pressure distribution  $P(x,s)$  over the free surface. This is now to be interpreted as "time"-varying pressure distribution imposed on a segment  $|x| < b(s)$  of the axis  $y=0$ , whose width  $2b(s)$  also varies with "time".

The solution is given by Wehausen and Laitone (1960, p. 615). It is convenient to write it in terms, not of the velocity potential  $\phi(x,y,s)$ , but rather of its conjugate, the stream function  $\psi(x,y,s)$ . In fact, since from now on we shall be concerned only with  $y=0$ , for brevity we write  $\psi(x,s)$  for  $\psi(x,0,s)$ . Thus

$$\rho U \psi(x,s) = \int_0^s d\sigma \int_{-b(\sigma)}^{b(\sigma)} d\xi P(\xi,\sigma) K(x-\xi,s-\sigma), \quad (3.6)$$

where

$$K(x,s) = \frac{1}{\pi} \int_0^\infty d\lambda \sin \lambda x \cos \sqrt{\frac{g\lambda}{U^2}} s \quad (3.7)$$

$$= \frac{1}{\pi x} F'(\omega) \quad (3.8)$$

with 
$$\omega^2 = \frac{gs^2}{4U^2|x|}, \quad (3.9)$$

and 
$$F'(\omega) = 1 + 2\omega \int_0^\omega d\zeta \sin(\zeta^2 - \omega^2) \quad (3.10)$$

$$= \frac{d}{d\omega} \int_0^\omega d\zeta \cos(\zeta^2 - \omega^2).$$

The function  $F'(\omega)$  can be expressed in terms of Fresnel integrals, e.g.

$$F'(\omega) = 1 + 2\omega\sqrt{\frac{\pi}{2}} \left\{ \cos \omega^2 S\left(\sqrt{\frac{\pi}{2}}\omega\right) - \sin \omega^2 C\left(\sqrt{\frac{\pi}{2}}\omega\right) \right\} \quad (3.11)$$

$$= 1 + 2\omega\sqrt{\frac{\pi}{2}} \left[ \frac{\cos\omega^2}{2} - \frac{\sin\omega^2}{2} - f\left(\sqrt{\frac{2}{\pi}}\omega\right) \right], \quad (3.12)$$

where  $S, C$  are Fresnel integrals, and  $f(\zeta)$  is an auxiliary function (Abramowitz and Stegun (1964), p. 300). The function  $F'(\omega)$  has convenient series and asymptotic expansions, respectively

$$F'(\omega) = 1 + \sum_{m=1}^{\infty} \frac{(-4\omega^4)^m}{1 \cdot 3 \cdot 5 \cdot \dots \cdot (4m-3) \cdot (4m-1)}, \quad (3.13)$$

which can be used for small  $\omega$ , and

$$F'(\omega) = \sqrt{\frac{\pi}{2}}\omega(\cos\omega^2 - \sin\omega^2) - \sum_{m=1}^{m_{\infty}} \frac{1 \cdot 3 \cdot 5 \cdot \dots \cdot (4m-3) \cdot (4m-1)}{(-4\omega^4)^m}, \quad (3.14)$$

which can be used for large  $\omega$ , for a suitable stopping point  $m_{\infty}$ .

The kernel  $K$  and function  $F'(\omega)$  occur also in classical Cauchy-Poisson problems (e.g. Lamb (1932), p. 384) and the physical description of the spreading waves produced is well-known. Indeed one can view the representation (3.6) as resulting physically from a "time" history of pressure pulses, the pulse  $P(x,s)$  at "time"  $\sigma=s$  being applied in order to cancel out instantaneously the spreading waves produced at earlier "times"  $\sigma < s$ . Our aim is to choose  $P(x,s)$  so that the stream function which is left over after this cancellation correctly satisfies the hull boundary condition. Somewhat similar ideas were used by Cummins (1956).

The boundary condition (2.5) is written in terms of  $\phi$ . However, using the Cauchy-Riemann equation  $\phi_y = -\psi_x$ , we have

$$\psi(x,s) = -U \int_0^x \eta_s(\xi,s) d\xi \quad (3.15)$$

Note that we have used the natural antisymmetry condition  $\psi=0$  at  $x=0$ . Thus once the hull shape  $\eta(x,s)$  is given,  $\psi(x,s)$  may be treated as a known function, and (3.6) then represents an integral equation to

determine the unknown pressure  $P(x,s)$ . For example, if the "ship" is a flat plate\* at an angle of attack  $\alpha$  then

$$\eta(x,s) = -\alpha s, \quad (3.16)$$

and we have immediately

$$\psi(x,s) = U\alpha s. \quad (3.17)$$

The analytical character of the integral equation (3.6) is of some interest. The equation is of Fredholm character with respect to the (space-like) variable  $x$  with dummy  $\xi$ , and of Volterra character with respect to the (time-like) variable  $s$  with dummy  $\sigma$  (Tricomi 1957). This means physically that information at all values of  $\xi$  is needed to determine the solution at any  $x$ , whereas only information at further forward stations  $\sigma < s$  is needed to determine the solution at a particular station  $s$ . We may hope to solve the equation in the  $s$ -dimension by a time-stepping or marching process, proceeding systematically from bow to stern, as in an initial-value problem for a differential equation. But at each station  $s$  we must expect to solve the Fredholm integral equation with respect to  $x$  in a manner more like a boundary-value problem for a differential equation.

Furthermore, the Fredholm equation in the  $x$  direction is singular. This is most apparent at  $g=0$ , where  $\omega=0$  and  $F'(\omega) = F'(0) = 1$ . Thus at  $g=0$ ,  $K(x-\xi, s-\sigma) = \frac{1}{\pi(x-\xi)}$ , and the  $\xi$ -integration is to be interpreted in the sense of Cauchy. In fact for any  $g \neq 0$  and  $\sigma \neq s$  the singularity is in a sense worse than the simple Cauchy pole, for as  $\omega \rightarrow \infty$  we have from (3.14)

$$F'(\omega) \rightarrow \sqrt{\frac{\pi}{2}} \omega (\cos \omega^2 - \sin \omega^2). \quad (3.18)$$

---

\*Or, in fact, any hull differing from that given by (3.16) by addition of a function of  $x$  alone, for example, a triangular section with a constant deadrise angle qualifies. Only the longitudinal slope  $\eta_s$  is hydrodynamically significant.

Thus as  $\xi \uparrow x$ ,

$$K(x-\xi, s-\sigma) \rightarrow \sqrt{\frac{g}{8\pi U^2}} (s-\sigma)(x-\xi)^{-3/2} \cos \left[ \frac{g(s-\sigma)^2}{4U^2(x-\xi)} + \frac{\pi}{4} \right]. \quad (3.19)$$

Hence if  $\sigma \neq s$ , the kernel function behaves like a "-3/2" power multiplied by a rapidly oscillating function, as  $\xi \rightarrow x$ . This behavior may be expected to cause some degree of numerical difficulty, and does.

Instead of tackling the integral equation for the pressure  $P$  itself directly, it is somewhat more convenient to work in terms of a function  $Q$  whose  $s$  derivative is  $P$ , namely

$$Q(x, s) = \int_{-\infty}^s P(x, \sigma) d\sigma. \quad (3.20)$$

Although the lower limit of (3.20) is written as " $-\infty$ ", it may equally well be replaced by zero, or in fact by  $s_0(x)$ , where  $s_0(x)$  is the station  $s$  at which  $x=b(s)$  i.e., the function  $s_0(x)$  is the mathematical inverse of the function  $b(s)$ . This is because  $P=0$  outside the hull projection on the plane  $y=0$ .

The function  $Q(x, s)$  is of course the loading on a unit-width strip of the hull at offset  $x$ , extending from the leading edge to station  $s$ . Hence, for example, the total lift force  $F_y$  in the  $y$  direction is obtained in terms of the values of  $Q$  at the trailing edge  $s=L$ , namely

$$F_y = \int_{-b(L)}^{b(L)} Q(x, L) dx. \quad (3.21)$$

More-complicated formulae involving  $Q$  at all stations  $s$  apply to the pitching moment and the drag. At infinite Froude number,  $Q$  is proportional to the velocity potential  $\phi$ ; specifically

$$Q = -\rho U \phi. \quad (3.22)$$

However, as is clear from the boundary condition (2.8), no such identification is possible if  $g \neq 0$ .

On substituting  $P(\xi, \sigma) = Q_\sigma(\xi, \sigma)$  in (3.6), and integrating by parts with respect to  $\sigma$ , we have

$$\rho U \psi(x, s) = \left[ \int_{-b(\sigma)}^{b(\sigma)} d\xi Q(\xi, \sigma) K(x-\xi, s-\sigma) \right]_{\sigma=0}^{\sigma=s} - \int_0^s d\sigma \int_{-b(\sigma)}^{b(\sigma)} d\xi Q(\xi, \sigma) K_\sigma(x-\xi, s-\sigma)$$

$$= \int_{-b(s)}^{b(s)} d\xi Q(\xi, s) K(x-\xi, 0) - \int_0^s d\sigma \int_{-b(\sigma)}^{b(\sigma)} d\xi Q(\xi, \sigma) K_{\sigma}(x-\xi, s-\sigma), \quad (3.23)$$

using  $Q=0$  at  $x=b(s)$ .

The first term of (3.23) involves  $K(x-\xi, 0)$  which is simply  $\frac{1}{\pi(x-\xi)}$ . Thus this term must be interpreted in the sense of Cauchy, and takes the form of a finite Hilbert transform (Tricomi, (1957), p. 173) which we write symbolically as

$$\mathcal{H}_{b(s)} Q(x, s) \stackrel{(\text{def})}{=} \frac{1}{\pi} \int_{-b(s)}^{b(s)} \frac{d\xi Q(\xi, s)}{x-\xi}. \quad (3.24)$$

Thus (3.23) becomes

$$\rho U \psi(x, s) = \mathcal{H}_{b(s)} Q(x, s) - \int_0^s d\sigma \int_{-b(\sigma)}^{b(\sigma)} d\xi Q(\xi, \sigma) K_{\sigma}(x-\xi, s-\sigma). \quad (3.25)$$

Equation (3.25) is the principal integral equation we shall attempt to solve. The kernel  $K_{\sigma}$  may, after some manipulation, be written in the form

$$K_{\sigma}(x-\xi, s-\sigma) = \frac{2}{\pi(s-\sigma)} \frac{\partial}{\partial \xi} F'(\omega) \quad (3.26)$$

where

$$\omega^2 = \frac{g(s-\sigma)^2}{4U^2|x-\xi|}. \quad (3.27)$$

Equation (3.25) agrees with the result of integrating Maruo's (1967) equation (57) with respect to (our)  $\xi$ , from  $\xi=0$  to  $\xi=x$ . Table 1 shows the equivalence of the various symbols used. Note that the function  $F(x, y)$  used by Maruo in his equation (58) et seq. was never defined, but is related to our  $K(x, s)$ . Maruo's equation (56), when similarly integrated with respect to (our)  $\xi$ , also agrees with our equation (3.6).

TABLE 1. EQUIVALENCE OF SYMBOLS

THIS PAPER	MARUO (1967)
$s, \sigma$	$x+l, x'+l$
$x, \xi$	$y, y'$
$y$	$z$
$\eta(x, s)$	$f(x, y)$
$P(x, s)$	$\rho U Y(x, y)$
$Q(x, s)$	$\rho U^2 g(x, y)$
$-\eta_s(x, s)$	$\omega(x, y)$
$\psi(x, s)$	$\int_0^y \omega(x, y') dy'$
$b(s)$	$bs(x/l)$
$B = 2b(L)$	$2b$
$L$	$2l$
$F$	$(2X_0)^{-1/2}$
$v$	$2X_0 l/b$
$F_Y$	$L$

#### 4. The High-Froude-Number Limit

The limit  $g \rightarrow 0$  may be carried out either on (3.6) or (3.25). In any case, if  $g=0$  the kernel  $K(x-\xi, s-\sigma) = \frac{1}{\pi(x-\xi)}$  is independent of  $s$  and  $\sigma$ . Hence in (3.25),  $K_{\sigma}=0$  and the integral equation reduces to

$$\mathcal{H}_b Q(x, s) = \rho U \psi(x, s). \quad (4.1)$$

There is now neither upstream nor downstream influence of the loading at one station on another, and the problem is solved immediately by inversion of the finite Hilbert transform, using the inverse Hilbert transform operator defined symbolically by

$$\mathcal{H}_b^{-1} = -(b^2-x^2)^{1/2} \mathcal{H}_b (b^2-x^2)^{-1/2}, \quad (4.2)$$

(Tricomi, 1957, p. 179).

Thus

$$\begin{aligned} Q(x, s) &= -\rho U (b^2-x^2)^{1/2} \mathcal{H}_b (b^2-x^2)^{-1/2} \psi(x, s) \\ &= -\frac{\rho U (b^2(s)-x^2)^{1/2}}{\pi} \int_{-b(s)}^{b(s)} \frac{d\xi \psi(\xi, s)}{(b^2(s)-\xi^2)^{1/2} (x-\xi)}. \end{aligned} \quad (4.3)$$

Normally the inverse operator  $\mathcal{H}_b^{-1}$  is not uniquely defined, and to any solution such as (4.3) we must add a multiple of the function  $(b^2-x^2)^{-1/2}$  whose Hilbert transform vanishes (Tricomi, (1957), p. 174). However, we can exclude this possibility in the present case, since this would generate velocity and pressure distributions with inverse 3/2 power singularities at the leading edge  $x=b(s)$ . In order to retain only integrable (inverse square root) pressure singularities, we must require a square-root zero in  $Q$ , leading to the solution (4.3).

Since  $Q$  is proportional to the velocity potential when  $g=0$ , the solution (4.3) could also have been obtained directly from the boundary-value problem with  $\phi=0$  as the free-surface condition, and simply expresses the fact that conjugate harmonic functions such as  $\phi$  and  $\psi$  are Hilbert transforms of each other on the  $x$ -axis. This solution is of course well known in aerodynamic low-aspect-ratio wing theory (see e.g. Newman & Wu, (1973). The solution for a flat plate is simply

$$Q(x,s) = \rho U^2 \alpha \sqrt{b^2(s) - x^2}, \quad (4.4)$$

the usual "elliptic loading distribution".

We are here interested rather in the first correction term to  $Q$ , resulting from finite-Froude-number effects. That is, we seek an asymptotic expansion for small  $g$  (or more correctly for small values of the appropriate normalized gravity parameter  $\nu = \frac{gL^2}{U^2B}$ ), which begins with a term  $Q=Q^\infty$  given by (4.3). Maruo (1967) has performed such an analysis on the lift coefficient in a special case and has proved that the first correction to the infinite-Froude-number lift is a factor of order  $\nu$ . That is, the asymptotic expansion at least begins like a Taylor series with respect to  $\nu$ .

A logical procedure for constructing this expansion is by successive approximation, i.e. since (4.3) resulted from dropping the last term of (3.25) entirely, the first correction to (4.3) is obtained by substitution of  $Q^\infty$  into this particular term. Thus if we put

$$Q = Q^\infty + Q^1 \quad (4.5)$$

where  $Q^1 \rightarrow 0$  as  $g$  or  $\nu \rightarrow 0$ , we have

$$\mathcal{H}_{b(s)} Q^1 = \int_0^s d\sigma \int_{-b(\sigma)}^{b(\sigma)} d\xi Q^\infty(\xi, \sigma) K_\sigma(x-\xi, s-\sigma). \quad (4.6)$$

While (4.6) may be a useful formula as it stands, we can simplify further, since  $K$  itself still depends on gravity  $g$ . But if for example we were to use the (truncated) series (3.13) to estimate  $K_\sigma$  for small  $g$ , we should only obtain terms of  $O(g^2)$ , not  $O(g)$  as expected from Maruo's analysis. Furthermore, the resulting integrals would diverge because of a non-integrable singularity at  $\xi=x$ . The highly-oscillatory behaviour of the kernel near  $\xi=x$ , as indicated by (3.19), suggests that the limit  $g \rightarrow 0$  needs special treatment, and it is clear by analogy with the method of stationary phase that only the neighborhood of  $\xi=x$  contributes significantly to the integral (4.6), to leading order.

Thus we expand  $Q^\infty$  in a Taylor series about  $\xi=x$ , giving



$$\mathcal{H}_b Q^1 = \int_0^s d\sigma \int_{\substack{\text{nbhd} \\ \text{of } x}} d\xi \left[ Q^\infty(x, \sigma) + (\xi-x) Q_x^\infty(x, \sigma) + \dots \right] K_\sigma \quad (4.7)$$

However,  $\xi$  can only take values near to  $x$  for  $s_0(x) < \sigma < s$  where  $s_0(x)$  is as defined below equation (3.20). Further, in view of (3.26), the term of (4.7) in  $Q^\infty(x, \sigma)$  integrates to zero, and we are left with

$$\mathcal{H}_b Q^1 = -\frac{2}{\pi} \int_{s_0(x)}^s d\sigma \frac{Q_x^\infty(x, \sigma)}{s-\sigma} \int_{x-\infty}^{x+\infty} d\xi (\xi-x) \frac{\partial}{\partial \xi} F'(\omega) \quad (4.8)$$

$$= -\frac{4}{\pi} \int_{s_0(x)}^s d\sigma \frac{Q_x^\infty(x, \sigma)}{s-\sigma} \int_0^\infty d\chi [F'(\omega) - 1], \quad (4.9)$$

where  $\chi = |\xi-x|$  and  $\omega^2 = \frac{g(s-\sigma)^2}{4U^2\chi}$ . On changing the variable of

integration from  $\chi$  to  $\omega$ , we have

$$\mathcal{H}_b Q^1 = \frac{2}{\pi} \frac{g}{U^2} \int_{s_0(x)}^s d\sigma (s-\sigma) Q_x^\infty(x, \sigma) \int_0^\infty \frac{F'(\omega) - 1}{\omega^3} d\omega \quad (4.10)$$

The last integral with respect to  $\omega$  is a pure constant, taking the value  $"-2\pi"$ . Thus, finally,

$$\mathcal{H}_b(s) Q^1(x, s) = -\frac{4g}{U^2} \int_{s_0(x)}^s d\sigma (s-\sigma) Q_x^\infty(x, \sigma) \quad (4.11)$$

The procedure for computing the leading-order gravity effects on the flow ( and in particular on the pressure distribution) is thus to compute first the infinite-Froude-number solution  $Q^\infty(x, s)$  by (4.3), substitute into (4.11), and then take a further inverse Hilbert transform to find  $Q^1(x, s)$ . Except in very special cases this procedure may be nearly as difficult as direct numerical solution of the integral equation (3.25). However, we note that the leading-order dependence on gravity  $g$  is linear, as is Maruo's (1967) estimate for the lift coefficient of a flat delta wing.

In the special case of the flat plate we may proceed a little further. Thus on use of (4.4) for  $Q^\infty$  in (4.11), we have

$$\mathcal{H}_b Q^1 = 4g\rho\alpha x \int_{s_0(x)}^s \frac{d\sigma(s-\sigma)}{\sqrt{b^2(\sigma)-x^2}} \quad (4.12)$$

It should be observed that the denominator vanishes at the lower limit  $\sigma=s_0(x)$  of the  $\sigma$  integration. In the further special case of a triangular waterplane

$$b(s) = \lambda s, \quad (4.13)$$

we can integrate (4.12) explicitly to give

$$\mathcal{H}_b Q^1 = 4g\rho \frac{\alpha}{\lambda} x \left[ s \log(s + \sqrt{s^2 - \frac{x^2}{\lambda^2}}) - \frac{1}{2} \sqrt{s^2 - \frac{x^2}{\lambda^2}} - s \log \frac{|x|}{\lambda} \right]. \quad (4.14)$$

Although no doubt the inverse Hilbert transform could now be obtained to generate Maruo's solution, our purpose here is rather to observe the remarkable introduction of singular behaviour along the center line  $x=0$ , as evidenced by the term of (4.14) in " $\log|x|$ ". This behaviour is characteristic of pointed flat plates. For example, if we consider the more general class of waterplanes whose behaviour near the bow is of the form

$$b(s) = \lambda s^n \quad (4.15)$$

for some positive exponent  $n$ , then the behavior of the integral (4.12) as  $x \rightarrow 0$  is of the form of an analytic function of  $x$ , plus a contribution of the order of  $s \cdot x^{1/n}$ ,  $n \neq 1$ , or  $s \cdot x \log x$ ,  $n=1$ .

Thus for all  $n \geq 1$ , the slope of the graph of the function  $\mathcal{H}_b Q^1$  against  $x$  is infinite at  $x=0$ . The function  $\mathcal{H}_b Q^1$  is of course an odd function of  $x$ .

The corresponding result for  $Q^1$  itself is that  $Q^1$  behaves like an analytic even function of  $x$ , plus a contribution of the order of  $s \cdot |x|^{1/n}$  for all  $n \neq 1/2$ , and  $s \cdot x^2 \log|x|$  for  $n=1/2$ . Specifically we have

$$Q^1(x, s) = Q^1(0, s) + \begin{cases} 0 (x^2), & 0 < n < 1/2 \\ s \cdot 0 (x^2 \log|x|), & n=1/2 \\ s \cdot 0 (|x|^{1/n}), & n > 1/2 \end{cases} \quad (4.16)$$

It should be noted that since  $P=Q_s$ , and the singular terms of (4.16) are linear in  $s$ , (4.16) indicates that the pressure distribution  $P$  itself has the same singular structure, with the strength of the singularities invariant along the length of the ship.

Thus for  $0 < n < 1/2$ , the pressure is well behaved, for  $n=1/2$  (blunt parabolic waterplane) the lateral pressure gradient vanishes at  $x=0$  but the lateral curvature of the graph of pressure against  $x$  is infinite, and similarly for  $1/2 < n < 1$ . For  $n=1$  (triangular waterplane) the lateral pressure gradient is discontinuous but finite at  $x=0$  while for all  $n > 1$  the lateral pressure gradient is infinite at  $x=0$ . That is, there is a very sharp but finite-magnitude pressure peak along the center line of any sharply-pointed flat plate.

The above result is of course essentially a gravitational effect, and stands in sharp contrast to the smooth behaviour of the elliptic loading (4.4) in the gravity-free case. The singularity is presumably due to the profound effect of the diverging waves generated at the extreme bow, whose wave length tends to zero along the track of the bow, irrespective of Froude number (Ursell, (1960)). Although the above analytic conclusions were obtained from a high-Froude-number expansion, it is probable that the essential character of the singularity is the same at all Froude numbers, and the numerical solution of section 7 tends to verify this. Experimental verification is eagerly awaited.

## 5. A Similarity Solution

We seek in the present section a solution  $P(x,s)$  of the integral equation (3.6) which has the same basic shape at all stations  $s$ . That is, the pressure distribution at any one station  $s$  is obtained from that at any other station by a simple scaling of  $P$  and  $x$ . The  $x$ -wise scale is obviously  $b(s)$ , and it is easy to see that the only possible multiplicative scale on  $P$  is some power of  $s$ . Thus we seek a solution of the form

$$P(x,s) = s^\gamma \tilde{P}\left(\frac{x}{b(s)}\right), \quad (5.1)$$

for some constant  $\gamma$  and some function  $\tilde{P}(x)$  of a single variable  $x$ .

Of course we have no guarantee that such a solution ever exists, and in particular could not expect it to exist without some special restriction on  $b(s)$ . In fact, we shall now show that (5.1) is a valid solution if and only if the waterplane consists of cusped parabolas, i.e. if

$$b(s) = \lambda s^2 \quad (5.2)$$

for some constant  $\lambda = B/2L^2$ . The body shape  $\eta(x,s)$  and thus the stream function  $\psi(x,s)$  will also possess a similarity character, and we shall verify that, for example,

$$\psi(x,s) = s^{\gamma-1} \tilde{\psi}\left(\frac{x}{b(s)}\right). \quad (5.3)$$

The above are the most general assumptions which permit a similarity solution. To verify that they are consistent, and to find the equation satisfied by  $\tilde{P}(x)$ , we substitute (5.1) and (5.3) into the integral equation (5.6).

Thus we have

$$\rho U s^{\gamma+1} \tilde{\psi}\left(\frac{x}{b(s)}\right) = \int_0^s d\sigma \sigma^\gamma b(\sigma) \int_{-1}^1 d\xi \tilde{P}(\xi) K(x-\xi b(\sigma), s-\sigma), \quad (5.4)$$

on substituting  $\xi = \xi b(\sigma)$ . Putting  $x = \tilde{x} b(s)$ , and using the form (3.8) of  $K$  gives

$$\rho U s^{\gamma+1} \tilde{\psi}(\tilde{x}) = \frac{1}{\pi} \int_0^s d\sigma \sigma^\gamma \int_{-1}^1 \frac{d\tilde{\xi}_P(\tilde{\xi})}{\mu \tilde{x} - \tilde{\xi}} F'(\omega) , \quad (5.5)$$

where

$$\mu = b(s)/b(\sigma) , \quad (5.6)$$

and

$$\omega^2 = \frac{g(s-\sigma)^2/b(\sigma)}{4U^2 |\mu \tilde{x} - \tilde{\xi}|} . \quad (5.7)$$

If we put  $\sigma=st$  in (5.5), we have

$$\rho U \tilde{\psi}(\tilde{x}) = \frac{1}{\pi} \int_{-1}^1 d\tilde{\xi}_P(\tilde{\xi}) \int_0^1 \frac{dt t^\gamma F'(\omega)}{\mu \tilde{x} - \tilde{\xi}} , \quad (5.8)$$

where now

$$\mu = b(s)/b(st) , \quad (5.9)$$

and

$$\omega^2 = \frac{gs^2(1-t)^2/b(st)}{4U^2 |\mu \tilde{x} - \tilde{\xi}|} . \quad (5.10)$$

So far, we have not made the assumption (5.2). In order that the original assumption (5.1) be valid it is necessary that (5.8) represent an integral equation for  $\tilde{P}(\tilde{x})$ , i.e. that it be independent of the station co-ordinate  $s$ . The parameter  $\mu$  is independent of  $s$  if and only if  $b$  is proportional to some power of  $s$ , while the parameter  $\omega$  is independent of  $s$  if and only if that power is exactly 2. Thus if (5.2) is satisfied, we have

$$\mu = t^{-2} , \quad (5.11)$$

and

$$\omega^2 = \frac{g(1-t)^2}{4\lambda U^2 |\tilde{x} - t^2 \tilde{\xi}|} = \frac{1}{2} v \frac{(1-t)^2}{|\tilde{x} - t^2 \tilde{\xi}|} . \quad (5.12)$$

Thus, finally, the integral equation for  $\tilde{P}(\tilde{x})$  can be written

$$\rho U \tilde{\psi}(\tilde{x}) = \int_{-1}^1 d\tilde{\xi}_P(\tilde{\xi}) K(\tilde{x}, \tilde{\xi}) , \quad (5.13)$$

where

$$\tilde{K}(\tilde{x}, \tilde{\xi}) = \frac{1}{\pi} \int_0^1 \frac{dt t^{\gamma+2}}{\tilde{x} - \tilde{\xi} t^2} F'(\omega) , \quad (5.14)$$

with  $\omega$  determined by (5.12).

The task of solving the one-dimensional integral equation (5.13) would appear to be considerably simpler than that of solving the general two-dimensional equation (3.6). However, the kernel  $\tilde{K}$  is obviously extremely complicated, and highly singular as  $\tilde{\xi} \rightarrow \tilde{x}$ . Hence numerical similarity solutions have so far been obtained only indirectly, via the general equation, and will be presented in section 7.

The quantity  $Q(x,s)$  whose  $s$  derivative is  $P$  also obeys a similarity law, of the form

$$Q(x,s) = s^{\gamma+1} \tilde{Q}\left(\frac{x}{b(s)}\right) . \quad (5.15)$$

On differentiation with respect to  $s$ , we establish the connection

$$P(\tilde{x}) = (\gamma+1) \tilde{Q}(\tilde{x}) - 2\tilde{x} \tilde{Q}'(\tilde{x}) \quad (5.16)$$

between the similarity profiles of  $P$  and  $Q$ . An integral equation for  $Q$  may also be obtained by substitution of (5.15) into (3.25), namely

$$\rho U \tilde{\psi}(\tilde{x}) = \tilde{H}_1 \tilde{Q}(\tilde{x}) + \int_{-1}^1 d\tilde{\xi} \tilde{Q}(\tilde{\xi}) \frac{\partial}{\partial \tilde{\xi}} \tilde{K}_1(\tilde{x}, \tilde{\xi}) , \quad (5.17)$$

where

$$\tilde{K}_1(\tilde{x}, \tilde{\xi}) = \frac{2}{\pi} \int_0^1 \frac{dt t^{\gamma+1}}{1-t} [F'(\omega) - 1] , \quad (5.18)$$

$\omega$  being given by (5.12) again.

The allowed shapes of the hull are of interest. Clearly we are allowed only the very specific cusped waterline prescribed by (5.2). However, considerably greater latitude is allowed in the shape of the cross-sections and some latitude is allowed in the longitudinal profile. Thus it is clear that the hull function  $\eta$  also has a similarity character, with

$$\eta(x,s) = s^\gamma \tilde{\eta}\left(\frac{x}{b(s)}\right) \quad (5.19)$$

The arbitrary exponent  $\gamma$  therefore characterizes the longitudinal profile or keel line, which is straight if  $\gamma=1$ , blunt if  $\gamma<1$  and cusped if  $\gamma>1$ \*. The case of a flat plate is included, with  $\gamma=1$  and  $\tilde{\eta}(x) = -\alpha = \text{constant}$ . More generally, any cross section shape defined by  $\tilde{\eta}(x)$  is allowed, but the hull shape must of course be similar for all stations, according to (5.19). The connection between the shape function  $\tilde{\eta}(x)$  and stream function  $\tilde{\psi}(x)$  may be obtained from (3.15), and we have

$$\tilde{\psi}(x) = 2\lambda U x \tilde{\eta}(x) - \lambda U (\gamma+2) \int_0^x \tilde{\eta}(\xi) d\xi \quad (5.20)$$

A physical justification of this similarity solution may be attempted as follows. At these high Froude numbers we are concerned only with the diverging part of the ship wave pattern near the ship's track, since the transverse wavelength  $2\pi U^2/g$  far exceeds the ship length. The diverging waves are (Ursell, (1960)) short in wavelength even for vanishing gravity, and in fact their crests asymptote to the axis  $x=0$  according to the parabolic law,  $x \sim s^2$ . Thus the growth of the waterplane (5.2) precisely matches the spreading of the diverging waves.

Given this physical picture we may speculate on the character of the solution, especially near the leading edges, for other waterplanes. For example, if the waterplane is more highly cusped than (5.2), i.e.  $n < 2$  in (4.15), the rate of spreading of waves exceeds the rate of growth of waterplane, and at some station the diverging waves must emerge from beneath the hull, changing fundamentally the character of the leading edge singularity and hence the spray sheet.

---

\* Remarkably, the special case  $\gamma=2$  allows similarity solutions with the non-linear free surface condition (2.6).

## 6. Numerical Procedure

In this section we discuss a procedure for numerical solution of the integral equation (3.25). The program used is quite unsophisticated, and further work is needed to develop more efficient programs. However, the accuracy attainable with the present method is satisfactory for some purposes.

The only numerical difficulty in solving (3.25) is with the double-integral term. Routines for efficiently inverting finite Hilbert transforms are easy to construct, so that the first term on the right of (3.25) gives no trouble. Notice that the double-integral term contains all "time"-history effects; that is, it and only it introduces an influence of previous stations  $\sigma < s$  on the pressure at the current station  $s$ . In this connection it is important to note that the kernel  $K_\sigma$  vanishes at the current station, ie. when  $\sigma = s$ .

We make use of this property in a "time"-stepping procedure, by first using the ordinary trapezoidal rule on the  $\sigma$ -integration. Having chosen a station spacing  $\Delta s$ , we write

$$Q_n(x) = Q(x, n\Delta s) \quad (6.1)$$

$$\psi_n(x) = \psi(x, n\Delta s) \quad (6.2)$$

$$b_n = b(n\Delta s) \quad (6.3)$$

and approximate

$$\rho U \psi_n(x) = \frac{1}{b_n} Q_n(x) - \Delta s \sum_{k=1}^{n-1} \int_{-b_k}^{b_k} d\xi Q_k(\xi) K_\sigma(x-\xi, (n-k)\Delta s) \quad (6.4)$$

Equation (6.4) can be written in the form of a recursive algorithm for  $Q_n$ , namely

$$Q_n(x) = \mathcal{H}_{b_n}^{-1} R_n(x) \quad (6.5)$$

where

$$R_n(x) = \rho U \psi_n(x) + \Delta s \sum_{k=1}^{n-1} \int_{-b_k}^{b_k} d\xi Q_k(\xi) K_\sigma(x-\xi, (n-k)\Delta s) \quad (6.6)$$



Note that  $R_n$  is determined from the known quantity  $\psi_n(x)$ , together with all  $Q_k(x)$ ,  $k=1,2,\dots,n-1$ , which are known at the  $n$ 'th step.

The next problem is evaluation of the  $\xi$ -integral in (6.6). We use a very crude estimate, in which  $Q_n(\xi)$  is taken as a constant, say  $Q_{jk}$ , on each of  $2M$  segments,  $j=\pm 1, \pm 2, \dots, \pm M$ , where the  $j$ 'th segment is defined by

$$\xi_{j-1} < \xi < \xi_j = b_k \sin \frac{j\pi}{2M} \quad (6.7)$$

Note that the same number  $2M$  of  $x$ -wise segments is used at every station  $s$ , the segment size increasing with waterplane width  $2b_k$ .

Using the formula (3.26) for  $K_\sigma$  and integrating explicitly with respect to  $\xi$ , we have

$$R_n(x) = \rho U \psi_n(x) - \frac{2}{\pi} \sum_{k=1}^{n-1} \frac{1}{n-k} \sum_{\substack{j=-M \\ j \neq 0}}^M Q_{jk} \left[ F'(\omega) \right]_{\xi=\xi_{j-1}}^{\xi=\xi_j} \quad (6.8)$$

with

$$\omega^2 = \frac{g(\Delta s)^2 (n-k)^2}{4U^2 |x-\xi|} \quad (6.9)$$

We now evaluate (6.8) at a point  $x=x_i$ , which is approximately the mid-point of the  $i$ 'th segment, namely

$$x_i = b_k \sin \frac{(i-\frac{1}{2})\pi}{2M}, \quad (6.10)$$

obtaining a set of values  $R_{in} = R_n(x_i)$ . Finally, a numerical inverse Hilbert transform, essentially evaluating an expression like (4.3) by the mid-point rule (after removing the Cauchy singularity), provides a corresponding set of values of  $Q_{in} = Q_n(x_i)$ . We now proceed to station  $n+1$ , etc. Note that no matrix manipulation (especially no inversion) is ever required in this method.

Difficulties arise because of the highly-singular nature of the kernel near  $\xi=x$ , as indicated by (3.19). Of course we never evaluate exactly at this point, and in obtaining (6.8) from (6.6) have integrated analytically through this singularity. Nevertheless, there is bound to be trouble in (6.8) due to large values of  $\omega$  whenever the point of evaluation  $x=x_i$  at some station  $s$  is close to an end point  $\xi=\xi_j$

of any segment at a previous station  $\sigma$ . Physically, each end point of a segment looks like an isolated singularity, which leaves its own "trail" in the form of wildly-oscillating waves (Ursell, (1960)). A better numerical method could be one in which the step-function character of  $Q_k(\xi)$  with  $\xi$  was replaced by a smoother variation, thereby moderating the apparent singularity.

This problem manifests itself in the form of apparently-random small fluctuations of  $R_n(x)$  as a function of  $x$ , superposed upon a "believable" smooth wave. It is cured in a not-altogether-satisfactory manner by two separate smoothing procedures. In the first place, we test each end point  $\xi_j$  while evaluating the sum (6.8) to ensure it is not too close to the current evaluation point  $x_i$ . If it is as close to  $x_i$  as 20% of the  $i$ th segment size, we shift  $x_i$  (staying within the  $i$ th segment) by that 20% amount. Secondly, after complete evaluation of the  $R_n(x_i)$ , we smooth by replacing  $R_n(x_i)$  by the mean of  $R_n(x_{i-1})$  and  $R_n(x_{i+1})$ .

The particular trigonometric lateral spacing (6.7) was chosen to provide a sufficient density of segments near the edges to counter the rapid (square-root) drop to zero of  $Q$ . In fact, explicit use is made of the nature of this spacing to make the inverse Hilbert transform most efficient, and for example the program reproduces exactly the result (4.4) for flat plates at infinite Froude number. However, this decision was made before the singular character of  $Q$  near the center plane was discovered. Actually the investigation of Section 4 was only carried out as a result of the appearance of the numerical results, and in retrospect it would appear that a greater density of points near the center plane would have been desirable.

## 7. Discussion of Computed Results

Figure 2 shows results for  $Q/\rho U^2 \alpha b(s)$  plotted against  $\tilde{x}=x/b(s)$  at various stations  $s$ , for the case of a flat plate with the cusped parabolic waterplane (5.2). This is the case in which a similarity solution exists, such that the quantity plotted should be independent of  $s$ . The results shown are for  $M=20$  and a maximum value of  $n=20$ , with the speed chosen so  $v=1.25$ . For example, with a length/beam ratio of 5.0, this would correspond to a conventional Froude number  $F=2.0$ .

We observe that at this fairly-high Froude number, a similarity profile is reasonably well achieved by about the mid-section of the ship. In fact departure from similarity very near the bow is inevitable, since the program starts with  $R_1(x) = 0$  in (6.5). That is, at the very first station  $n=1$  there is an apparent infinite-Froude-number or zero-gravity solution, irrespective of the actual Froude number. This is shown as the  $s=0$  curve in Figure 2, and is simply the elliptic loading (4.4). The behavior for the first few stations is quite erratic, but the oscillations apparently die out as  $s$  increases.

If we now vary  $v$ , i.e. vary the Froude number, we obtain the family of similarity profiles shown in Figure 3. These are essentially plots of  $\tilde{Q}(\tilde{x})$ , as in (5.15) with  $\gamma=1$ . However, they are actually obtained as in Figure 2 from the general program at  $s/L=1.0$ . Similarity is harder to achieve numerically as  $v$  increases, i.e. as the effect of gravity increases, especially near the center plane. The curves are dashed wherever an uncertainty of more than about 5% exists, and discontinued altogether as soon as the uncertainty reaches 10%.

Corresponding curves of the actual pressure  $\tilde{P}(\tilde{x})$  could be obtained from (5.16), but the necessary numerical differentiation would reduce the accuracy of the results unacceptably. However, it is clear that the general character is of a sharp but finite pressure peak at the center plane, with a pressure minimum about half-way out, followed by an infinite positive-amplitude (inverse-square-root) peak at the edge  $\tilde{x}=1$ . This infinity corresponds to the leading-edge spray sheet.

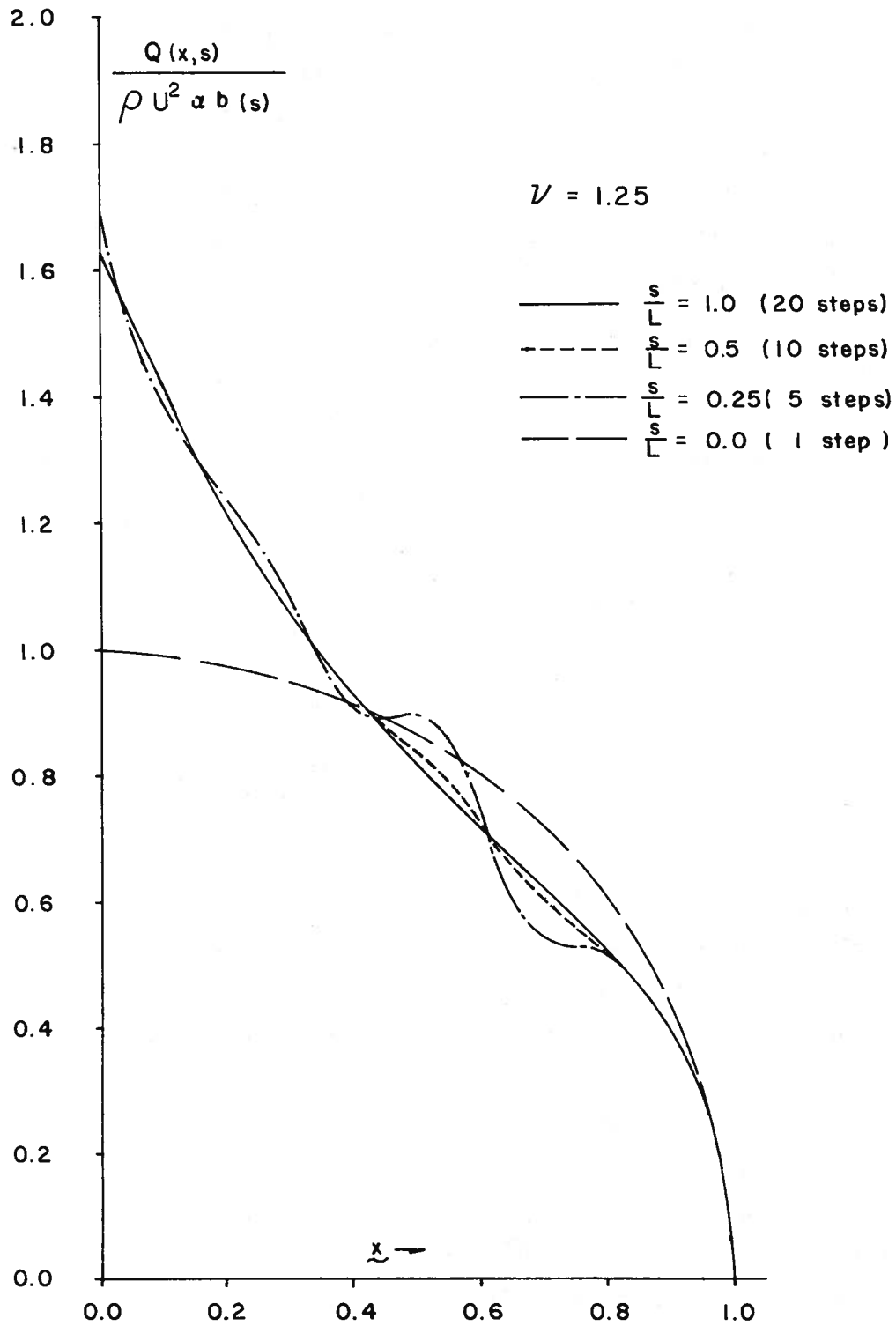


Figure 2: Similarity check for cusped waterplane. Scaled loading distribution at various stations, for fixed  $\nu = gL^2/U^2B$

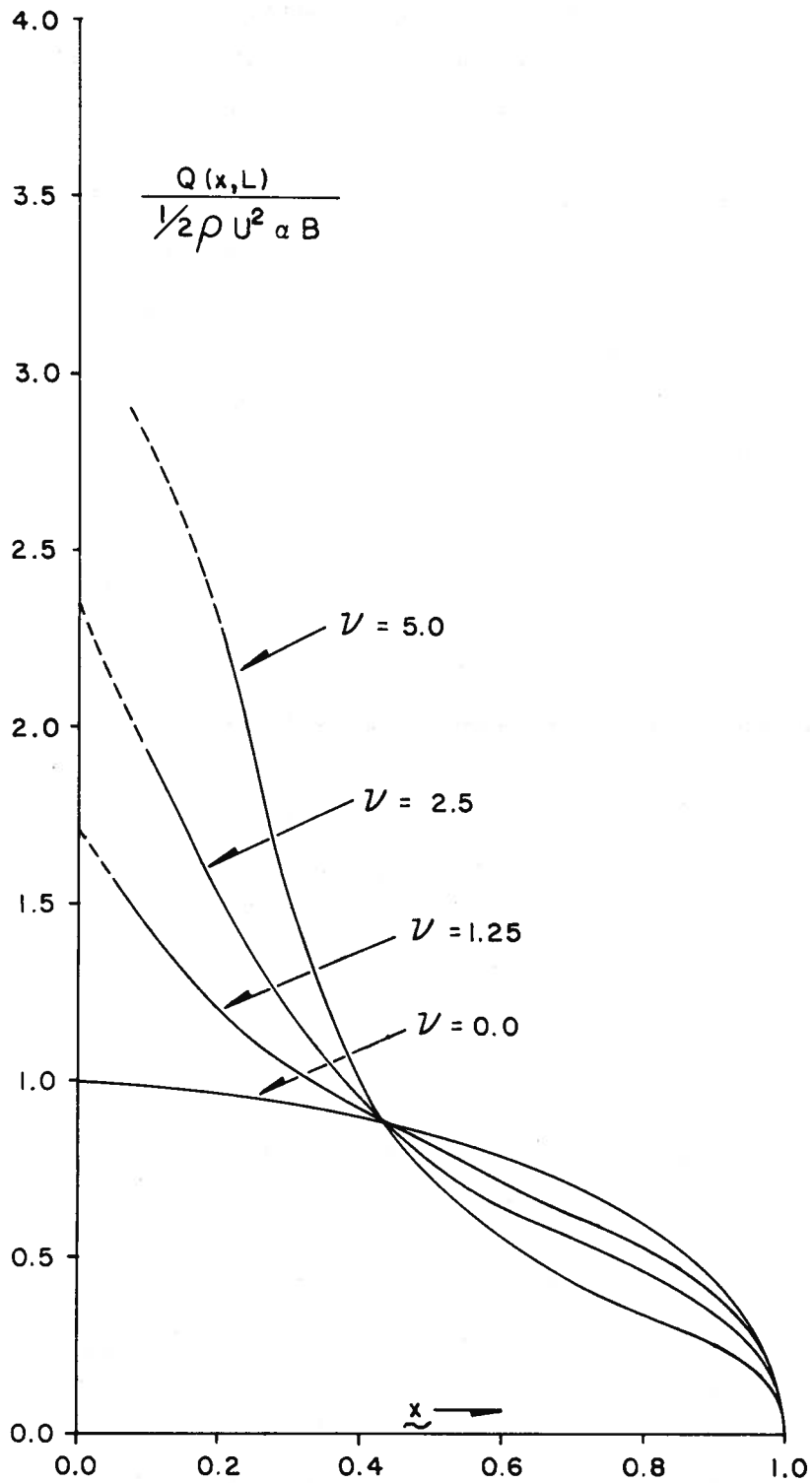


Figure 3: Trailing edge loading distribution for cusped waterplane at various values of  $\nu = gL^2/U^2B$

Figure 4 shows the loading  $Q$  at the trailing edge  $s/L=1.0$  for the case of a triangular waterplane, i.e. for a delta wing, at various values of  $\nu$ . The results are analogous to those of Figure 3, but the profiles are no longer self-similar with respect to  $s$ . On the contrary, Figure 4 has an alternative interpretation as a plot of scaled loadings at various stations  $s$  for a fixed value of  $\nu$ . For example, at  $\nu=2.5$  the loading at the mid-section  $s/L=0.5$  is precisely half of the result shown in Figure 3 for the trailing-edge loading at  $\nu=1.25$ .

In both Figures 3 and 4 the center-plane singularity suggested by the analysis of Section 4 is qualitatively evident. Unfortunately, program accuracy in this region is, not surprisingly, least satisfactory, so that we are not able to verify the differences in the actual degree of singularity, as indicated by (4.16).

Perhaps a more significant difference between Figures 3 and 4 is in the strength of the pressure singularity at the edge  $\tilde{x}=1$ , which appears approximately invariant with  $\nu$  for the similarity profiles of Figure 3. In the case of the delta wing, however, there appears to be a real weakening of the pressure singularity as  $\nu$  increases, or as we move from bow to stern at fixed  $\nu$ . In fact for all  $\nu > 2.1$  the computer program predicts small negative loadings very near to  $\tilde{x}=1$ . Since this implies a negative infinity in the pressure, it is not a physically-acceptable result. Unfortunately it is hard with the present crude program to tell whether these are genuine theoretical predictions, or numerical errors. However, the fact remains that no such negative values are ever obtained in the similarity case of Figure 3.

This effect is anticipated by the discussion at the end of Section 5, and we can illustrate it more strongly by use of the even-blunter waterplane  $n=1/2$  in (4.15), i.e. one which is parabolic in  $s$  against  $x$ . Figure 5 shows loadings for this case. There is now no doubt from the computer output that for  $\nu > 1.1$  the predicted edge loading is negative. What actually happens here is not clear; what is clear, however, is that the present theory is no longer valid. Note also from Figure 5 that for this blunt body, the center-plane singularity has almost disappeared and the pressure gradient now appears to vanish at  $\tilde{x}=0$ , as predicted by Section 4.

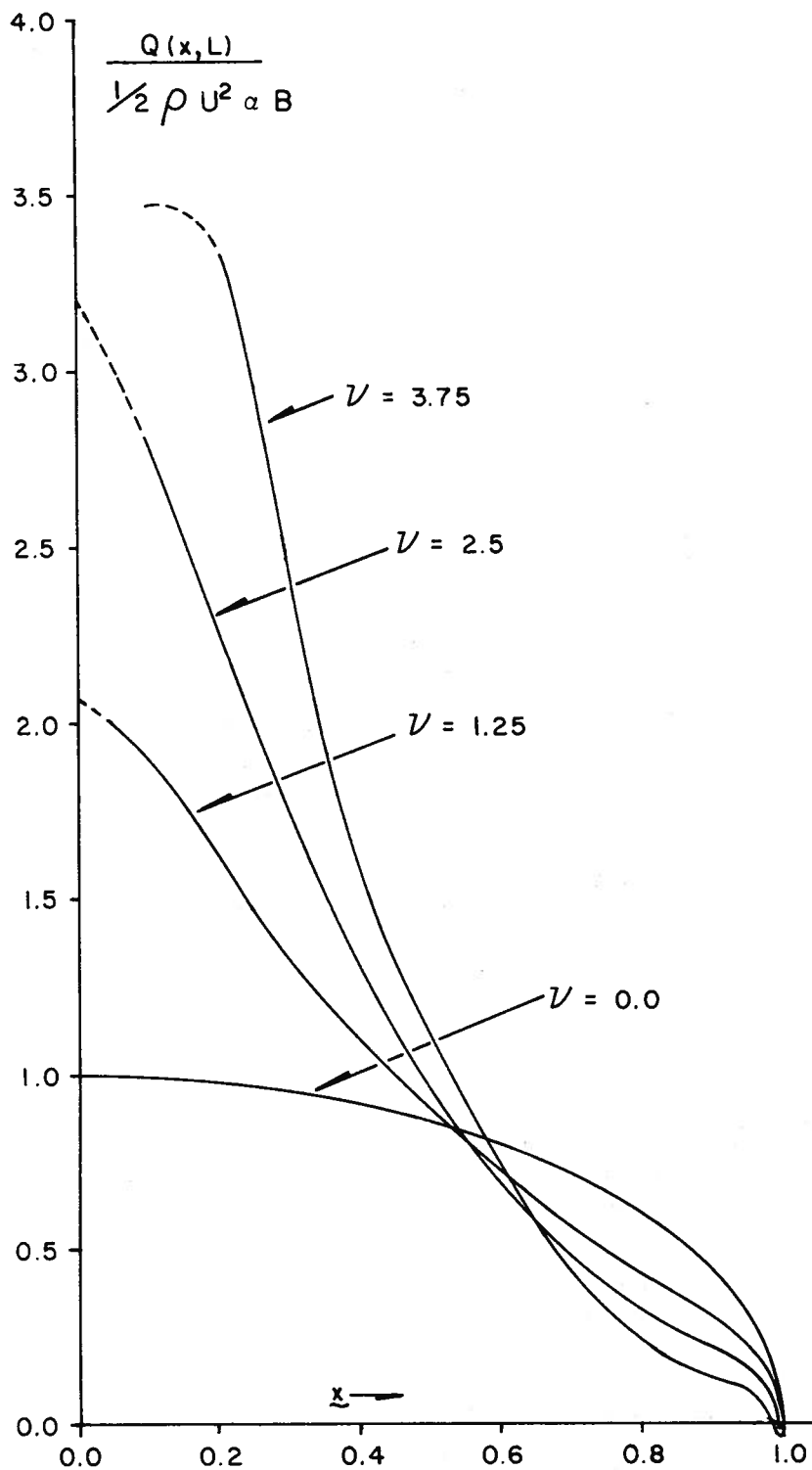


Figure 4: Trailing edge loading distribution for triangular (delta wing) waterplane, at various values of  $\nu = gL^2 / U^2 B$

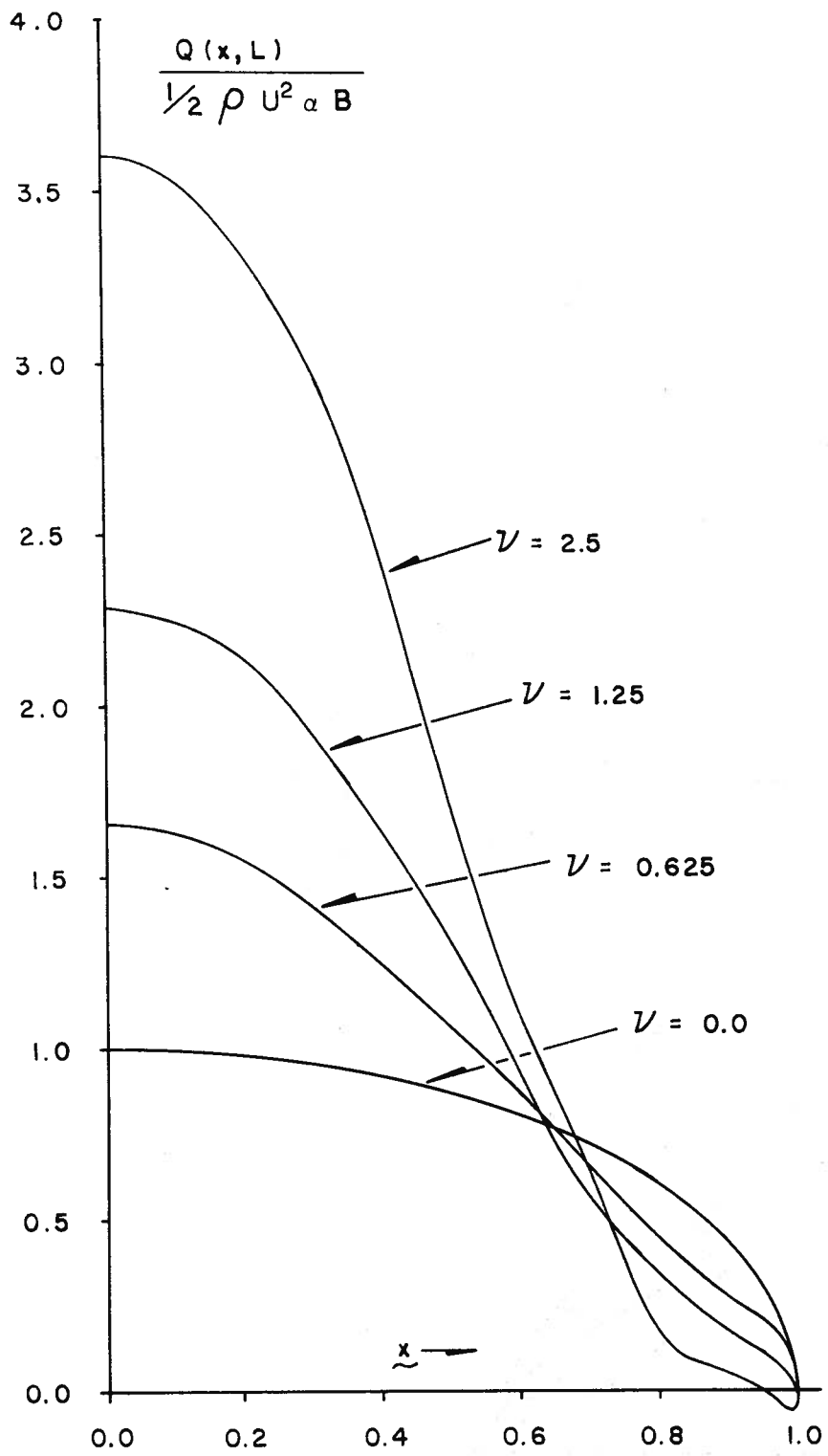


Figure 5: Trailing edge loading distribution for blunt waterplane at various values of  $\nu = gL^2/U^2B$



Figure 6 shows the variation with  $\nu$  of the lift force  $F_y$ , computed according to (3.21) and scaled with respect to the infinite-Froude-number (i.e.  $\nu=0$ ) value

$$F_y^\infty = \frac{\pi}{2} \rho U^2 \alpha [b(L)]^2 \quad . \quad (7.1)$$

Results for all three waterplanes discussed above are shown. For the triangular case only, comparison may be made with Maruo's (1967) very-high-Froude-number approximation

$$F_y / F_y^\infty = 1 + 0.211\nu \quad , \quad (7.2)$$

a straight line which clearly gives the correct asymptotic behavior for small  $\nu$  .

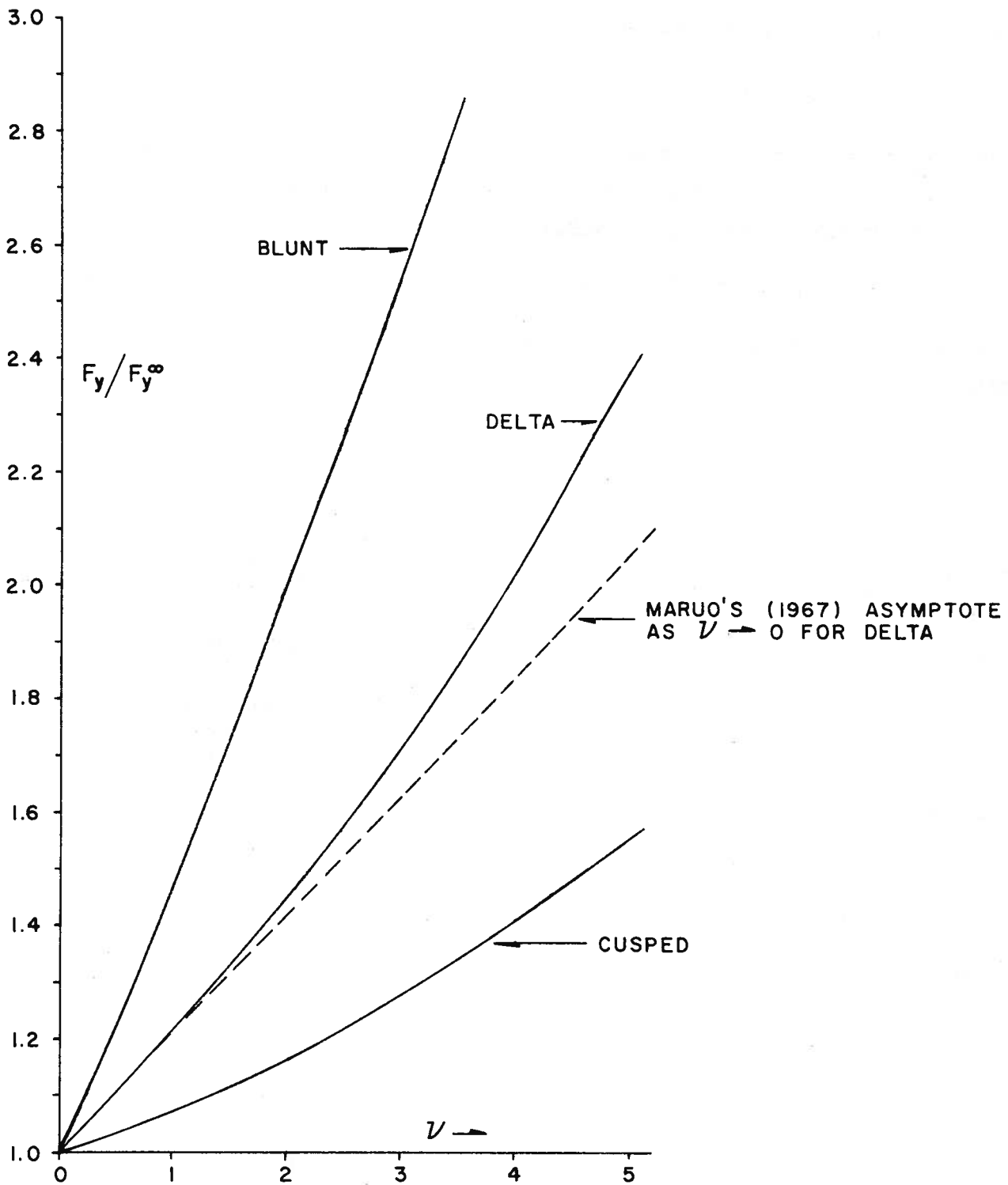


Figure 6: Lift of various flat plates, scaled with respect to the zero-gravity limit, and plotted against  $v = gL^2/U^2 B$ .

## References

- ABRAMOWITZ, M. & STEGUN, L.A. (eds), "Handbook of Mathematical Functions", Washington, National Bureau of Standards, 1964.
- ACOSTA, A.J. & DE LONG, R.K., "Experimental Investigation of Non-steady forces on Hydrofoils Oscillating in Heave", I.U.T.A.M. Symp. on Non-Steady Flow of Water at High Speeds, Leningrad, 1971.
- CUMMINS, W.E., "The Wave Resistance of a Floating Slender Body", Ph.D. Thesis, American University, 1956.
- GADD, G., "A Method for Calculating the Flow Over Ship Hulls", Trans. R.I.N.A., 112 (1970) 335.
- GILBARG, D. "Jets and Cavities", Handbuch der Physik, Volume 9, Springer, 1960.
- HAVELOCK, T.H., "The Theory of Wave Resistance", Proc. Roy. Soc. Lond. (A) 138 (1932) 339-348 (collected works, p. 367).
- LAMB, H., "Hydrodynamics", 6th edn., Cambridge & Dover, 1932.
- MARUO, H., "High-and Low-Aspect Ratio Approximation of Planing Surfaces", Schiffstechnik, 72 (1967), 57-64.
- MICHELL, J.H. "The Wave Resistance of a Ship", Phil. Mag (5) 45 (1898), 106-123.
- MONACELLA, V.J. & NEWMAN, J.N., "The Pressure on the Sea Bottom Due to a Moving Pressure Distribution", N.S.R.D.C. Report 2308, Department of the Navy, Washington, D.C., 1967.
- NEWMAN, J.N. & WU, T. Y-T., "A Generalized Slender-Body Theory for Fish-like Forms", J. Fluid Mech., 1973.
- OGILVIE, T.F., "Non-linear High-Froude-Number Free-Surface Problems," J. Engin. Math. 1 (1967), 215-235.
- VAN OORTMERSSEN, G., "Some Aspects of Large Offshore Structures", 9th Symp. on Naval Hydro., Paris, 1972.
- ROGALLO, R.S., "A Trailing-Edge Correction for Subsonic Slender-Wing Theory", Ph.D. Thesis, Stanford University, 1969.
- TRICOMI, F.G., "Integral Equations", Interscience, 1957.
- TUCK, E.O., "A Systematic Asymptotic Expansion Procedure for Slender Ships", J. Ship Res., 8 (1964), 15-23.
- TUCK, E.O. & VON KERCZEK, C., "Streamlines and Pressure Distribution on Arbitrary Ship Hulls at Zero Froude Number", J. Ship Res., 12 (1968), 231-236.

TULIN, M.P., "The Theory of Slender Surfaces Planing at High Speeds",  
Schiffstechnik, 4 (1956) 125-133.

URSELL, F., "On Kelvin's Ship Wave Pattern", J. Fluid Mech., 8 (1960)  
418-431.

WANG, D.P., & RISPIN, P., "Three-Dimensional Planing at High Froude  
Number", J. Ship Res., 15 (1971), 221-230.

APPENDIX: *Computer Program Listing*

MAIN PROGRAM

```

C   LCW ASPECT RATIO FLAT SHIP THEORY
C   COMPUTES LOADING Q (=STATICWISE PRESSURE INTEGRAL) AND THE
C   RESULTING LIFT COEFFICIENT FOR SHIPS OF SMALL DRAFT AND BEAM
C   REFERENCE: MARUD 1967, TUCK 1974
C
      DIMENSION R(50),QQ(50),PSI(50,50),DX(50)
      COMMON XM(50), SX(50),M,DPHIOP,A(50),TT(50),G,XX(50),Q(50,50),TPDT
C
C   M = NUMBER OF LATERAL POINTS (OFFSETS,BUTTOCKS) IN A HALF-WIDTH
C   OF THE SHIP. NOTE: SAME FOR ALL STATIONS. SPACING IS SQUARE ROOT
C   BIASSED TOWARD EDGE, SCALED WRT HALF BEAM A(J) AT STATION J .
C   N = NUMBER OF STATIONS, EQUALLY SPACED
C
      READ (5,9) M,N
      9 FORMAT(2I10)
      WRITE(6,21) M,N
      21 FORMAT(4H1 M=,I4,3H N=,I4,///,32H J   TT(J)   A(J)   PSI(J,K))
      EM = M
      DPHIOP = 0.5/EM
      DPHI = 3.1416 * DPHIOP
      HDPHI = 0.5 * DPHI
      DO 2 K = 1,M
      PHI = K*DPHI
      XX(K) = SIN(PHI)
      PHI = PHI - HDPHI
      XM(K) = SIN(PHI)
      SX(K) = COS(PHI)
      DX(K) = SX(K) * DPHI
      2 CONTINUE
C
C   PRESENT PROGRAM GENERATES HULL DATA INTERNALLY FOR FLAT DELTA
C   WING,HALF APEX "ANGLE"=0.1, ANGLE OF ATTACK "SLOPE"=0.1, SO THAT
C   THE HALF WATERPLANE WIDTH IS A(J) = 0.1 * TT(J) . TT IS THE
C   STATION COORD, GUES FROM 0 TO 1 . GENERALISATION TO MORE GENERAL
C   WATERPLANES IS EASY; JUST REPLACE DEFINING STATEMENT FOR A(J) .
C   GENERALISATION TO OTHER THAN FLAT PLATE REQUIRES MORE EFFORT, SEE
C   TUCK 1974, TO SET UP MATRIX OF STREAM FUNCTION PSI(J,K)
C
      SLOPE = 0.1
      ANGLE = 0.1
      DT = 1./N
      TPDT = 0.63661 * DT
      AREAWP = 0.
      DO 105 J = 1,N
      TT(J) = DT * J
      A(J) = ANGLE * TT(J)
      AREAWP = AREAWP + A(J)
      DO 100 K = 1,M
      100 PSI(J,K) = SLOPE * XM(K)*A(J)
      105 WRITE(6,106) J,TT(J),A(J),(PSI(J,K),K = 1,M)
      106 FORMAT(I6,12F9.5)
      AREAWP = 2.*DT*(AREAWP-0.5*A(N))
      WPCCEF = 0.5 * AREAWP / A(N)
      ASPECT = (4. * A(N)**2 ) / AREAWP
      BL = 2. * A(N)

```

Main Program (continued)

```
WRITE(6,61) BL,ASPECT,WPCOEF
61 FORMAT(14H BEAM/LENGTH =,F8.4,15H ASPECT RATIO =,F8.4,19H WATERPLA
LINE COEFF =,F8.4)
```

```
C
C INPUT VALUES OF  $G=1/F^{**2}$  , F=FROUDE NO. BASED ON LENGTH.
C NEGATIVE G HAS EFFECT OF ZERO G (INFINITE F )
C ZERO INPUT G VALUE (THAT IS,BLANK CARD) STOPS PROGRAM
C
```

```
10 READ(5,11) G
11 FCRMAT (F10.5)
   IF(G) 12,13,14
12 WRITE(6,15)
15 FCRMAT (5H1 G=0)
   G = 0.
   GO TO 17
14 FROUDE = 1./SQRT(G)
   WRITE(6,16) G,FROUDE
16 FCRMAT(4H1 G=,F6.3,7HFROUDE=,F6.3)
17 WRITE(6,63)
63 FCRMAT(26H  Q(J,1)  Q(J,2)  ETC      )
   DO 101 J = 1,N
   CALL FLAT(J,R)
   CALL SMOOTH(R)
   DO 102 K = 1,M
102 R(K) = PSI(J,K) - R(K)
   CALL HILBIN(QQ,R)
   DO 44 K = 1,M
   44 Q(J,K) = QQ(K)
101 WRITE(6,103) (Q(J,K),K=1,M)
103 FCRMAT(10F10.5)
   CLIFT = 0.
   DO 60 K = 1,M
   60 CLIFT = CLIFT + Q(N,K) * DX(K) * A(N)
   CLIFT = 4. * CLIFT / AREAWP
   WRITE(6,62) CLIFT
62 FCRMAT(F10.5)
   GO TO 10
13 STOP
   END
```

End of Main Program. Listings follow for Subroutines FLAT, SMOOTH,  
HILBIN and FPRIM2.

```
      SUBROUTINE FLAT(N1,R)
C   EVALUATES R(J) , AS IN TUCK 1974
      DIMENSION R(50)
      COMMON XM(50), SX(50),M,DPHIOP,A(50),TT(50),G,XX(50),Q(50,50),TPDT
      DO 5 KK = 1,M
        5 R(KK) = 0.
      IF(N1-1) 100,100,101
101 IF(G) 100,100,102
102 N = N1 - 1
      XCLD = - A(N1) * XM(1)
      DO 3 KK = 1,M
        X = A(N1) * XM(KK)
C
C   THIS IS A CRITICAL DECISION CARD. DXCRIT IS THE CRITICAL
C   CLUSENESS BETWEEN THE CURRENT FIELD POINT AND THE TRACK OF A
C   PREVIOUS PRESSURE PCINT. THE NUMBER "0.2" USED IS RATHER ARBITRARY
C   VALUES OF 0.1 AND 0.3 GIVE SIMILAR RESULTS.
      DXCRIT = 0.2 * (X - XCLD)
      SUMOUT = 0.
      DC 2 J = 1,N
        T = TT(N1) - TT(J)
        SUMIN = 0.
        WNUM = 0.25 * G * T**2
        FKOLD = 0.
        DC 1 K = 1,M
          XI = A(J) * XX(K)
          AX = ABS(X-XI)
C   HERE IS WHERE DXCRIT IS USED. IF "AX" IS BELOW DXCRIT, WE SIMPLY
C   REPLACE IT BY DXCRIT, THUS CALLING THE FRESNEL INTEGRAL ROUTINE
C   WITH A SUBSTANTIALLY REDUCED ARGUMENT. A VERY ROUGH TRICK
          IF(AX.LT.DXCRIT) AX = DXCRIT
          WMNUS2 = WNUM/AX
          WPLUS2 = WNUM/(X+XI)
          FKERN = FPRIM2(WMNUS2) - FPRIM2(WPLUS2)
          SUMIN = SUMIN + Q(J,K) * (FKERN - FKOLD)
        1 FKCLD = FKERN
        2 SUMOUT = SUMOUT + SUMIN/T
          XCLD = X
        3 R(KK)=TPDT*SUMOUT
100 RETURN
      END
```

```
      SUBROUTINE SMOOTH(R)
C   SMOOTHS R BY REPLACING CLD R WITH THE AVERAGE OF ITSELF AND
C   WHAT WE GET BY LINEAR INTERPOLATING BETWEEN THE 2 NEAREST VALUES.
      COMMON XM(50), SX(50),M,DPHIOP,A(50),TT(50),G,XX(50),Q(50,50),TPDT
      DIMENSION R(50), RN(50)
      M1 = M-1
      DO 1 J = 2,M1
        JM = J - 1
        JP = J + 1
        D = 1. / (XM(JP) - XM(JM) )
        AM = ( XM(J) - XM(JM) ) * D
        AP = ( XM(J) - XM(JP) ) * D
        1 RN(J) = AM * R(JP) - AP * R(JM)
        RN(M) = ((1. - XM(M) ) / (1. - XM(M1) ) ) * R(M1)
      DO 2 J = 2,M
        2 R(J) = 0.5 * ( R(J) + RN(J) )
      RETURN
      END
```

```
      SUBROUTINE HILBIN (Q,R)
C INVERSE HILBERT TRANSFORMER, USES MID PT RULE
C OUTPUT Q AT SAME (COSINE) SPACINGS AS INPUT R
C SPACINGS MUST BE COSINE, THAT IS SQUARE ROOT BIAS TO ENDS
C ASSUMES ANTISYMMETRY OF INPUT R , SYMMETRY OF OUTPUT Q , ABOUT
C CENTERLINE X = 0. USES ONLY POSITIVE X'S, BUILDS IN SYMMETRIES.
      COMMON XM(50), SX(50), M,DPHIUP
      DIMENSION F(50), R(50), Q(50)
      DC 1 L = 1,M
      SUM = 0.
      DC 2 K = 1,M
      IF ( K - L ) 3,2,3
3 F(K) = (R(L)-R(K))/(XM(L)-XM(K)) + (R(L)+R(K))/(XM(L)+XM(K))
2 CONTINUE
      IF(L-1) 4,4,5
4 F(1) = 2.*F(2) - F(3)
      GO TO 8
5 IF(L-M) 6,7,7
7 F(M) = 2.*F(M-1) - F(M-2)
      GO TO 8
6 F(L) = 0.5 * (F(L-1) + F(L+1) )
8 DC 9 K = 1,M
9 SUM = SUM + F(K)
1 Q(L) = DPHIUP * SX(L) * SUM
      RETURN
      END
```

```
      FUNCTION FPRIM2(WW)
C FRESNEL INTEGRAL ROUTINE
      DOUBLE PRECISION ZZ,DD,TER,FPRIM
      IF(WW-16.) 1,2,2
1 ZZ = - 4. * WW**2
      FPRIM = 1.
      TER = 1.
      DO 3 M = 1,500
      MM = 4 * M - 1
      DD= MM * (MM-2)
      TER = TER * ZZ/ DD
      FPRIM = FPRIM + TER
      IF(CABS(TER) - 0.000001) 4,3,3
3 CONTINUE
4 FPRIM2 = FPRIM
      RETURN
2 W = SQRT(WW)
      Z = -4. * WW**2
      SUM = 1.
      TERM = 1.
      DO 5 M = 1,20
      MM = 4 * M - 1
      D = MM * (MM-2)
      TERM = TERM * D / Z
      SUM = SUM + TERM
      IF(ABS(TERM) - 0.000001) 6,5,5
5 CONTINUE
6 FPRIM2 = 1. - SUM + 1.253314 * W * (COS(WW) - SIN(WW))
      RETURN
      END
```



The University of Michigan, as an equal opportunity/affirmative action employer, complies with all applicable federal and state laws regarding nondiscrimination and affirmative action, including Title IX of the Education Amendments of 1972 and Section 504 of the Rehabilitation Act of 1973. The University of Michigan is committed to a policy of nondiscrimination and equal opportunity for all persons regardless of race, sex, color, religion, creed, national origin or ancestry, age, marital status, sexual orientation, gender identity, gender expression, disability, or Vietnam-era veteran status in employment, educational programs and activities, and admissions. Inquiries or complaints may be addressed to the Senior Director for Institutional Equity and Title IX/Section 504 Coordinator, Office of Institutional Equity, 2072 Administrative Services Building, Ann Arbor, Michigan 48109-1432, 734-763-0235, TTY 734-647-1388. For other University of Michigan information call 734-764-1817.